# Dynamics of temporal attention revealed by continuous tracking of visual cortical responses

Rachel N. Denison[1,2]*†, Karen Tian[1,2]†, David J. Heeger[1], Marisa Carrasco[1]
[1]New York University, [2]Boston University
†These authors contributed equally to this work

**Corresponding author:**
Rachel N. Denison
rdenison@bu.edu

Department of Psychological and Brain Sciences
Boston University
64 Cummington Mall
Boston, MA 02215
United States

**Keywords:** temporal attention, temporal expectation, magnetoencephalography, steady state visual evoked response

## Abstract

We can often anticipate the precise moment when a stimulus will be relevant for our behavioral goals. Voluntary attention, the prioritization of sensory information at relevant time points, enhances visual perception, but the underlying neural mechanisms are unknown. To determine whether and how voluntary temporal attention dynamically modulates visual cortical activity, we continuously tracked visual cortical responses using a flickering noise stimulus and MEG recording while human observers performed a temporal attention task. We found two neural signatures of voluntary temporal attention: First, cortical response reliability gradually ramped up in anticipation of the predictable onset of visual targets, with the slope of the ramp modulated by temporal attention. Second, the impact of a target on the cortical response to the flicker was larger when that target was temporally attended. These data reveal how temporal attention dynamically modulates visual cortical responses to prioritize sensory information at precise moments.

## Introduction

We can often anticipate the points in time at which sensory events will be relevant for our behavioral goals. For example, when returning a tennis serve, it is critical to see the ball at the moment it hits your opponent's racket; only seeing the ball half a second earlier or later would be unhelpful. This prioritization of sensory information at specific points in time is temporal attention. In the case of the tennis serve, we attend in a goal-directed manner to the relevant time point, an example of voluntary temporal attention.

Voluntary temporal attention affects behavior by both improving perceptual sensitivity and speeding reaction times to attended stimuli (*1*–*9*). However, the neural mechanisms underlying these perceptual improvements are unknown. One possibility is that temporally precise changes in perceptual sensitivity arise from time-varying attentional modulation of sensory areas (*6*, *10*). But whether and how voluntary attention to a point in time dynamically modulates sensory signals is unknown.

Previous neural studies have not isolated the impact of temporal attention on sensory responses while controlling for other possible time-varying processes. Studies have typically manipulated temporal attention –the relevance of an upcoming stimulus time– together with temporal expectation –the predictability of an upcoming stimulus time. However, attention and expectation can and should be distinguished. Studies in visual spatial and feature-based attention, as well as in audition, have shown that relevance and predictability can have distinct behavioral and neural effects (*11*–*21*). In the domain of visual temporal attention, we have found that voluntary temporal attention improves performance (*6*–*8*) and affects microsaccades (*22*) over and above the effects of expectation. These results also suggest dissociable neural mechanisms for temporal attention and expectation.

A commonly observed neural signature of expectation is a slow ramping activity, increasing over the course of hundreds of milliseconds to several seconds, that peaks around the time of an anticipated event. A variety of ramping signals have been observed in dorsal stream cortical and subcortical areas (*23*–*26*). Gamma band ramping signals were observed in V1 leading up to an expected time (*27*), but ramping in sensory areas has rarely been investigated.

In contrast to a gradual ramp, our normalization model of dynamic attention, which was fit to psychophysical data (*6*–*8*), predicts that voluntary temporal attention changes the gain of visual responses rapidly and transiently, roughly coincident with the evoked sensory response to the visual stimulus (*6*). A slow ramping modulation of visual responses may not allow such temporally precise attentional selection.

Here we investigated how temporal attention dynamically modulates visual cortex using MEG. Human observers performed a challenging perceptual task in which voluntary temporal attention was manipulated independent of temporal expectation. A precue directed attention to one of two sequential targets that were presented at fixed, predictable times. To measure attentional modulation continuously across time, we presented a 20 Hz flickering noise patch throughout each trial, which generated a steady-state visual evoked response (SSVER) at 20 Hz in the visual cortex (*28*, *29*). We tracked time-resolved visual cortical responses throughout the trial by calculating the inter-trial phase coherence (ITPC) at the stimulus frequency. ITPC is the primary driver of SSVER power (*28*–*31*) and indexes the reliability with which the visual stimulus drives cortical responses.

We found dynamic task-related modulations of visual cortical responses leading up to and following target stimuli. Behaviorally, orientation discrimination improved when the precue directed attention to the target time. In the neural data, visual cortical ITPC slowly ramped up in

anticipation of the predictable target stimuli regardless of the precue, an overall effect of temporal expectation. Voluntary temporal attention had two, separate effects on visual cortical ITPC. First, temporal attention modulated the slope of the ramp, with a steeper slope when the first of the two targets was attended. Second, temporal attention selectively increased the transient ITPC response to the first target when it was attended, changing the relative response magnitudes for the two targets according to the attentional precue. The results unify previous findings by showing how both ramping and transient modulatory mechanisms contribute to temporal attention. The presence and timecourse of these dynamic modulations in visually-driven cortical activity suggest a mechanism for how temporal attention can selectively enhance visual perceptual sensitivity at specific moments in time.

## Results

### Temporal precueing improved perceptual sensitivity

To investigate the effects of voluntary temporal attention on visual cortical dynamics, we recorded MEG while observers performed a temporal attention task with fully predictable stimulus timing (**Figure 1**). Observers (n = 10 x 2 sessions) directed temporal attention to one of two sequential grating targets separated by a 300 ms stimulus onset asynchrony (SOA) and discriminated the orientation of one grating on each trial. A precue tone before the targets instructed observers to attend to either the first target (T1) or second target (T2), and a response cue tone after the targets instructed observers to report the tilt (clockwise or counterclockwise) of one of the targets. The response cue matched the precue with 75% validity, so observers had incentive to direct their attention to different points in time according to the precue.

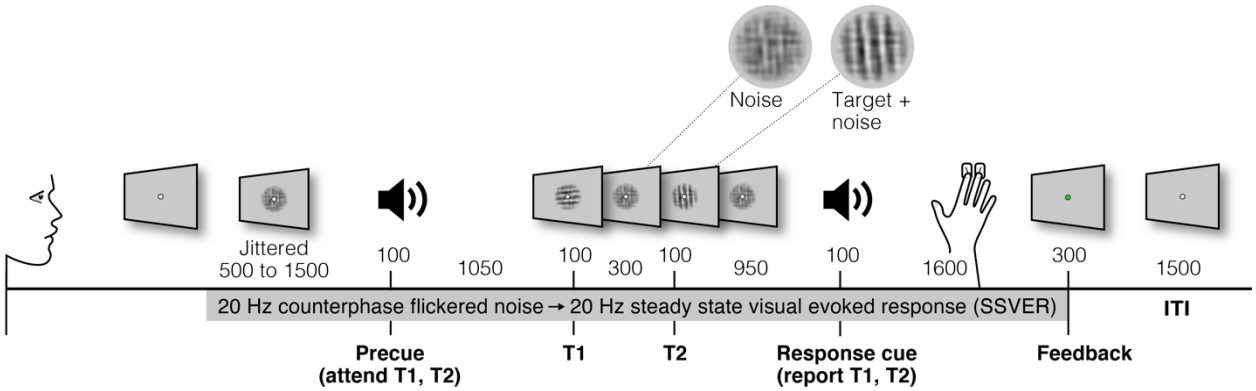


**Figure 1.** Temporal cueing task. Trial timeline showing stimulus durations and SOAs in ms. Targets were embedded in 20 Hz counterphase flickering noise. Precues and response cues were pure tones (high = cue T1, low = cue T2).

Temporal attention improved orientation discrimination performance, consistent with previous findings (*4–8*). Perceptual sensitivity (*d'*) was higher overall for valid trials (when the response cue matched the precue) than invalid trials (when the response cue did not match) (main effect of validity: F(1,9) = 8.03, *p* = 0.02,  = 0.25) (**Figure 2**). Perceptual sensitivity for T1 was higher than that for T2 (main effect of target: F(1,9) = 16.47, p = 0.0028,  = 0.261). No other main effects or interactions were found for *d'* (F(1,9) < 3.05, p > 0.11). Given the directional nature of time, we also tested how temporal attention affected each target separately. The improvement in *d'* with temporal attention was significant for T1 individually (F(1,9) = 9.08, *p* = 0.01,  = 0.38; valid: mean *d'* = 1.79, SD = 0.44; invalid: mean *d'* = 1.21, SD = 0.88) with a trend for improvement for T2 (F(1,9) = 4.75, *p* = 0.06,  = 0.20; valid: mean *d'* = 1.20, SD = 0.39; invalid: mean *d'* = 0.85, SD = 0.61). Reaction time (RT) was faster for valid versus invalid trials overall (F(1,9) = 39.87, *p* < 0.001, = 0.76) and for each target individually ([T1: F(1,9) = 43.02, *p* < 0.001,  = 0.79; valid: mean RT =

0.62 s, SD = 0.23 s; invalid: mean RT = 0.89 s, SD = 0.23 s] ,[T2: F(1,9) = 34.71, $p < 0.001$, = 0.74; valid: mean RT = 0.63 s, SD = 0.24 s; invalid: mean RT = 0.88 s, SD = 0.22 s]). No other main effects or interactions were found for RT (F(1,9) < 2.66, p > 0.14) (**Figure 2**). Thus, we can rule out any speed-accuracy tradeoffs in the effect of the precue on performance.

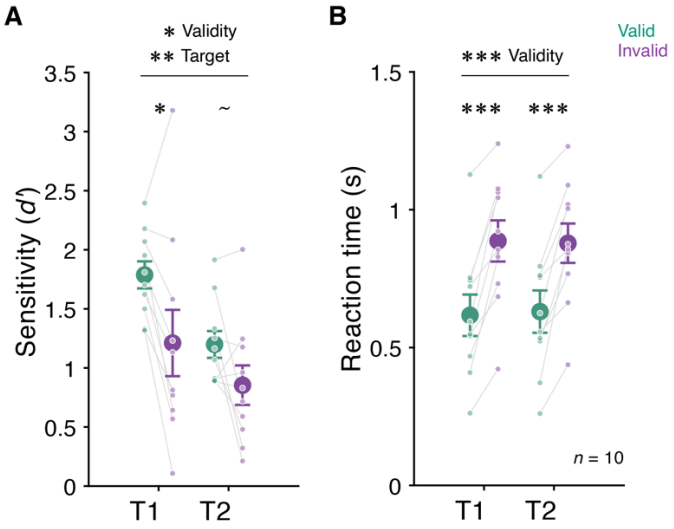


**Figure 2.** Behavior. Mean (**A**) perceptual sensitivity and (**B**) reaction time for each target (T1, T2) by attention condition. Sensitivity was higher and reaction time faster for valid (green) than invalid (purple) trials. Error bars indicate ± 1 SEM. ~ p < 0.1; * p < 0.05; ** p < 0.01; *** p < 0.001.

### Continuous tracking of visual responses using ITPC

To allow continuous tracking of visual responses as observers deployed temporal attention, we used an SSVER protocol. The grating targets were embedded in a stream of 20 Hz counterphase flickering noise, filtered to have similar orientation and spatial frequency content as the targets. The targets were presented superimposed on the noise background for 100 ms each and also flickered at 20 Hz in phase with the ongoing noise flicker. This protocol allowed visual cortical responses to be tracked throughout the trial by measuring the 20 Hz SSVER.

For each observer, we first measured the 20 Hz SSVER power for each channel, calculated from the average time series across all trials (henceforth “trial-average power”), and selected the five most visually responsive channels for further analysis. As expected, the most visually responsive channels were located in the back of the head, consistent with occipital responses (**Figure 3A**). We confirmed strong 20 Hz trial-average power in these channels and found that power was enhanced specifically at the 20 Hz stimulus frequency (**Figure 3C**).

Trial-average power depends on two factors: 1) single-trial power and 2) phase coherence across trials at the frequency of interest, or ITPC (**Figure 3B**). Therefore, we next asked how the 20 Hz SSVER depended on these two factors. As in previous studies that have pulled apart ITPC and single-trial power (*28–31*), we found that ITPC was the dominant component of the trial-average SSVER, with a strong and specific 20 Hz ITPC response (**Figure 3E**). Single-trial power had a relatively weak 20 Hz component and was dominated by alpha power around 10 Hz (**Figure 3D**). We therefore used ITPC as our primary measure to quantify responsiveness to visual stimulation in our subsequent analyses.

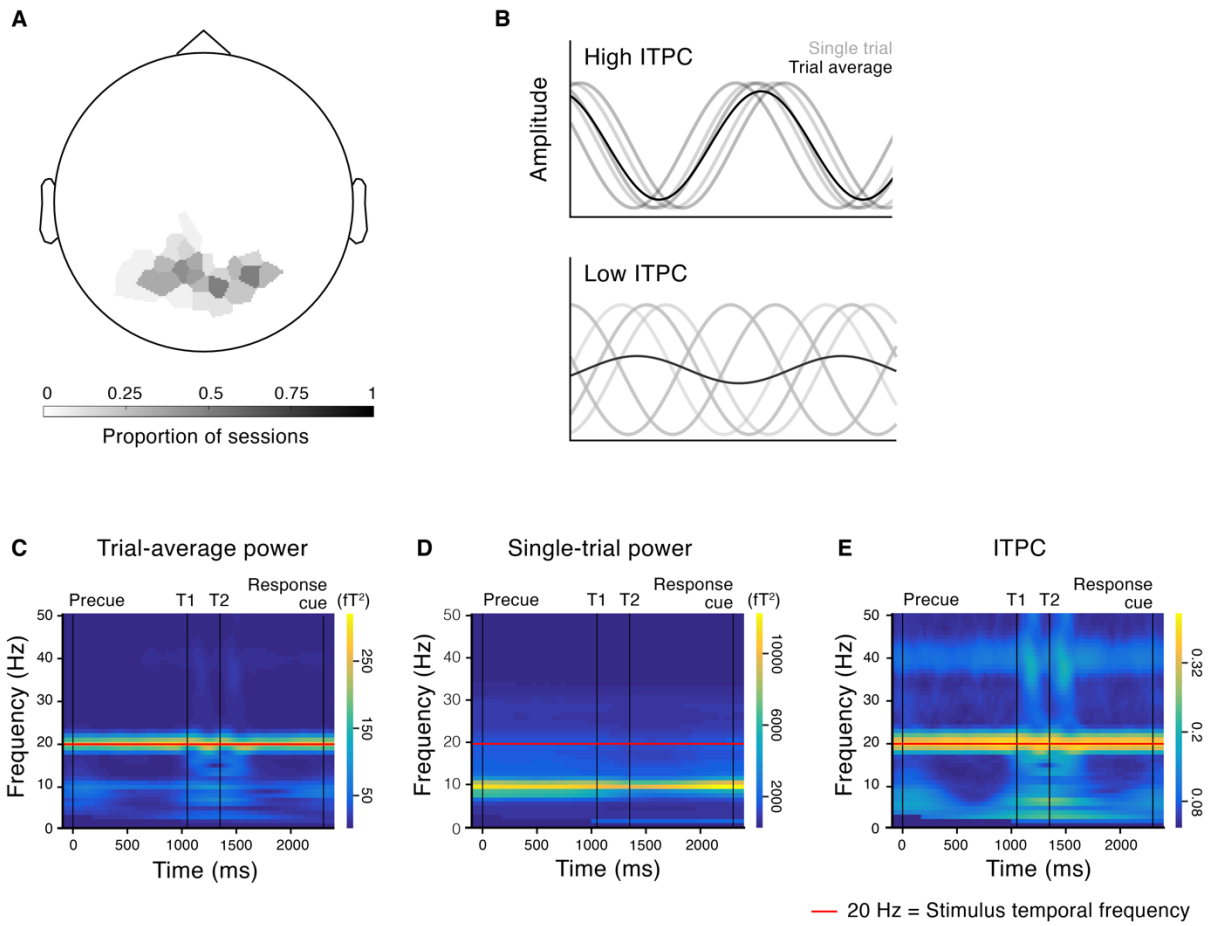


**Figure 3.** MEG responses to steady-state visual stimulation. (**A**) Topography of visually responsive channels across observers (top five channels selected for each session based on 20 Hz trial-average SSVER power). Grayscale indicates the proportion of sessions across observers in which the channel was selected as visually responsive. (**B**) Illustration of cartoon time series from five trials (gray) and their average (black). High phase coherence across trials results in high ITPC and trial-average power (top); low phase coherence across trials results in low ITPC and trial-average power (bottom), despite the same single-trial power. (**C-E**) Time frequency spectrograms of (**C**) trial-average power reveals a strong 20 Hz signal at the stimulus frequency. Trial-average power depends on two factors: (**D**) the power on single trials and (**E**) phase coherence across trials, or ITPC. The trial-average power at 20 Hz was more strongly reflected in ITPC than in single-trial power.

### Temporal expectation was accompanied by a ramping increase in ITPC

We first asked how temporal expectation affected ITPC in the period between the precue and the first target. In all trials, a predictable interval of 1.05 s elapsed between the onset of the precue and the onset of T1, so observers could form an expectation about the timing of T1 onset regardless of which target was precued to be attended (*7*, *8*, *22*). We observed an apparent neural signature of expectation in the form of a slow ramping increase of ITPC (mean slope = 0.045 ΔITPC/s, SD = 0.043) during the precue-to-T1 period (**Figure 4A, Supplementary Figure 1**). To quantify the rate of increase, we fit lines to each observer's ITPC time series from the onset of the precue to 80 ms before T1 (a cushion before T1 was inserted to prevent responses to T1 from interfering with the fit, see Methods). The slope of the ITPC time series was positive for 8/10 observers and significantly greater than zero across the group ($F(1,9) = 3.31$, $p = 0.009$, $= 0.40$) (**Figure 4B**). In contrast, single-trial power showed no ramping increase in the precue-to-T1

period (**Supplementary Figure 1C**), confirming that a ramping increase in cortical response reliability was the critical factor driving the change in ITPC.

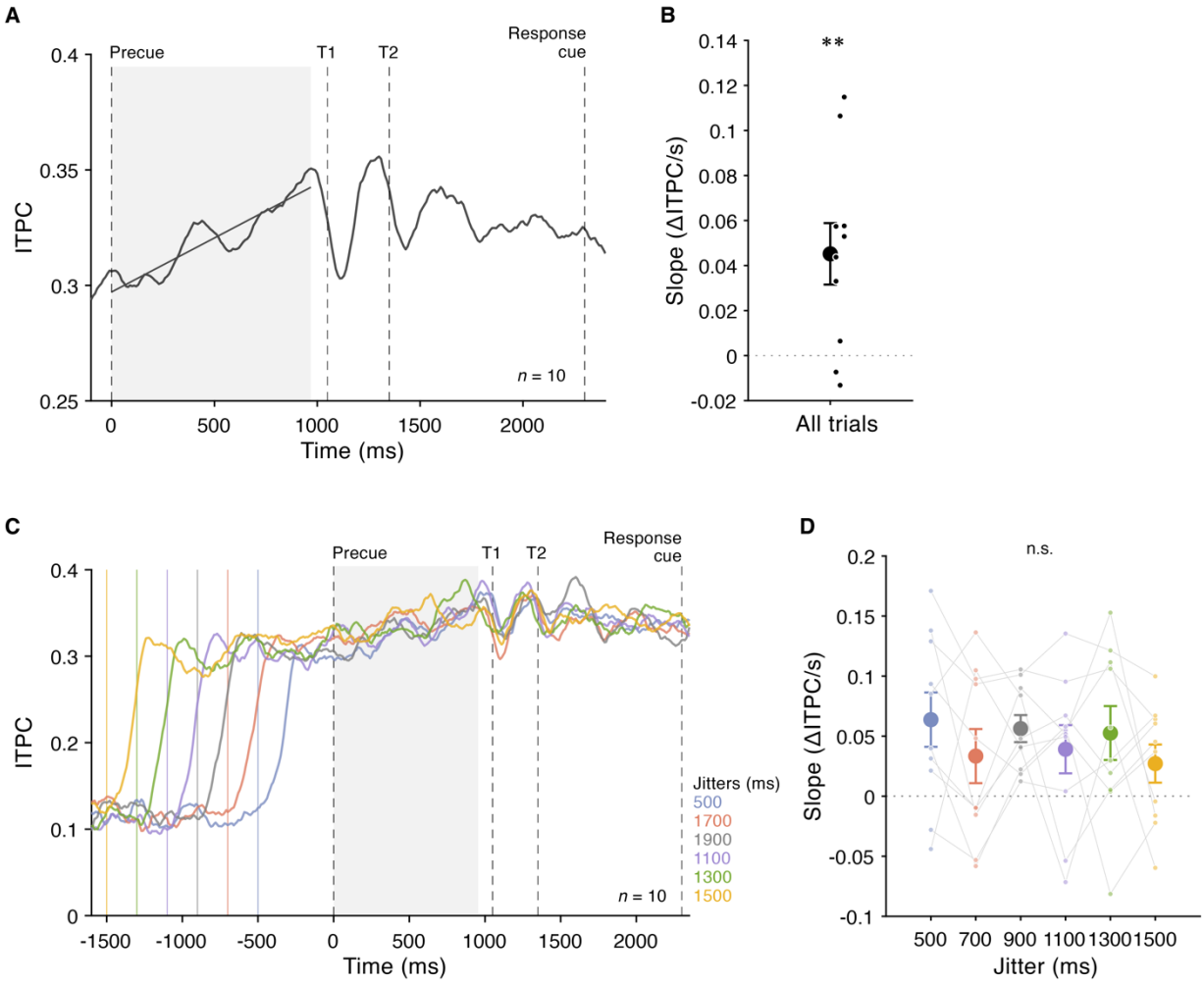


**Figure 4.** Ramping increase in ITPC associated with temporal expectation. (**A**) Mean 20 Hz ITPC time series across all trials ($n$ = 10). Lines were fit to each observer's ITPC time series during the precue-to-T1 period (gray shading). Linear fit to group data (gray line) shown for visualization. (**B**) Fitted slopes for each observer and group mean. (**C**) ITPC ramp is time-locked to the precue. Mean 20 Hz ITPC time series ($n$ = 10) for each jittered duration of SSVER stimulation before the precue. Colored vertical lines indicate the onset of the stimulus flicker for each duration. (**D**) ITPC slopes during the precue-to-T1 period were similar for all jitter durations. Large data points show the group means, and small data points show individual data, with each observer's data points connected by lines. Error bars are ±1 SEM. ** $p < 0.01$ compared to zero.

To ensure this ITPC ramp was locked to the precue and not simply the continuous build-up of the SSVER signal, we separated trials according to the duration of the SSVER stimulation period before the precue, which had been jittered from 500 to 1500 ms to prevent predictable precue timing. A one-way ANOVA revealed no significant differences in ITPC slope across the six jitter durations ($F(1,9) = 1.19$, $p = 0.30$, $= 0.03$). (**Figure 4C,D**). Therefore, the ITPC ramp was evidently initiated by the precue and indicates a gradual increase in visual cortical response reliability tied to temporal expectation.

### Temporal attention modulated the rate of anticipatory ramping of ITPC

We next asked whether temporal attention—over and above expectation—affects the anticipatory increase in ITPC as the target onset time approaches. Whereas expectation reflects the predictability of visual events, attention incorporates the task-relevance of events (*6*, *7*, *16*, *17*, *22*). In the present experimental design, temporal expectation was constant across all trials, because the two targets always appeared at the same, predictable times. Temporal attention, however, varied with the precue.

We therefore asked whether the precue affected the ramping response reliability in advance of the targets. To do so, we fit lines to each observer's ITPC time series during the precue-to-T1 period, with separate fits for precue T1 and precue T2 trials. (Note that we could only characterize ramping signals before T1, because the interval between T1 and T2 is short and contains the evoked response to T1.) We found that the slope was steeper for precue T1 trials (mean slope = 0.058 ΔITPC/s, SD = 0.057) than for precue T2 trials (mean slope = 0.032 ΔITPC/s, SD = 0.049). The magnitude of the difference in slope was 56% of the overall rate of increase and reliable across observers ($F(1,9) = 7.60$, $p = 0.022$, $= 0.16$). This result indicates that temporal attention acts over and above expectation to modulate anticipatory ramping of ITPC depending on the timing of upcoming task-relevant targets (**Figure 5**).

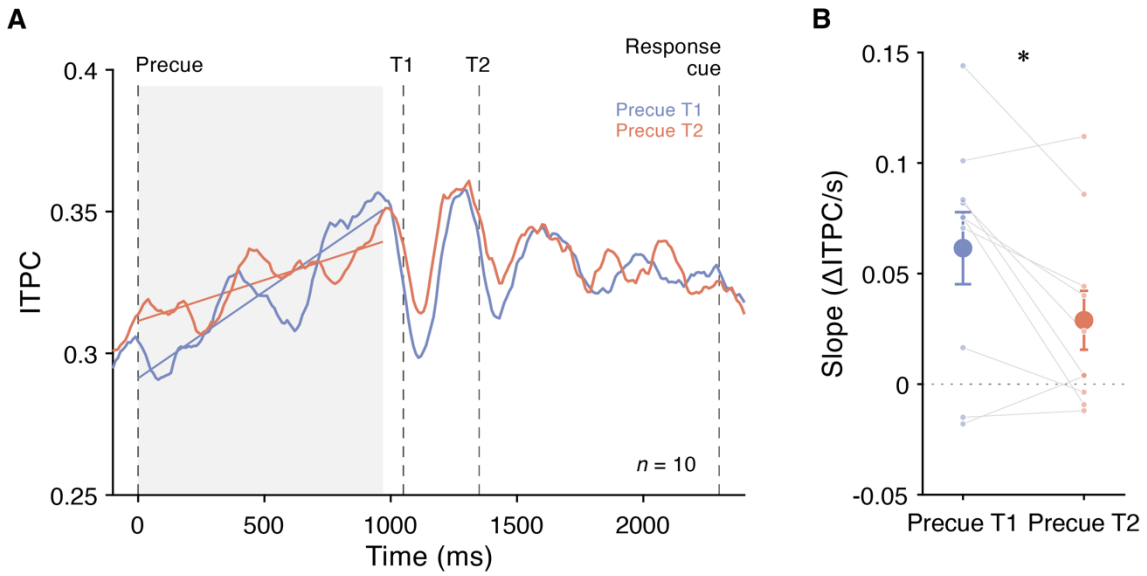


**Figure 5.** Anticipatory effect of precue on ITPC. (**A**) Mean 20 Hz ITPC time series for each precue type (*n* = 10). Lines were fit to each observer's ITPC time series during the precue-to-T1 period (gray shading). Linear fits to group data (red and blue lines) shown for visualization. (**B**) Temporal attention affected the ramping ITPC leading up to the first target. Fitted slopes were larger for precue T1 trials (blue) than for precue T2 trials (red). Error bars indicate ± 1 SEM. * $p < 0.05$.

### Temporal attention transiently affected the target-evoked ITPC response

We next asked how temporal attention affected the ITPC response to the targets. A target stimulus briefly superimposed on an SSVER stimulus can either enhance or suppress the ongoing SSVER, such that some observers show transient increases (upward peaks) in the SSVER signal following the target stimulus whereas others show transient decreases (downward peaks) (**Supplementary Text**). Thus, we asked how temporal attention affected the magnitude of this target-evoked ITPC

response for each observer using a normalized measure of ITPC (see Methods). The group average normalized ITPC time series has clear peaks after each target (**Figure 6A**).

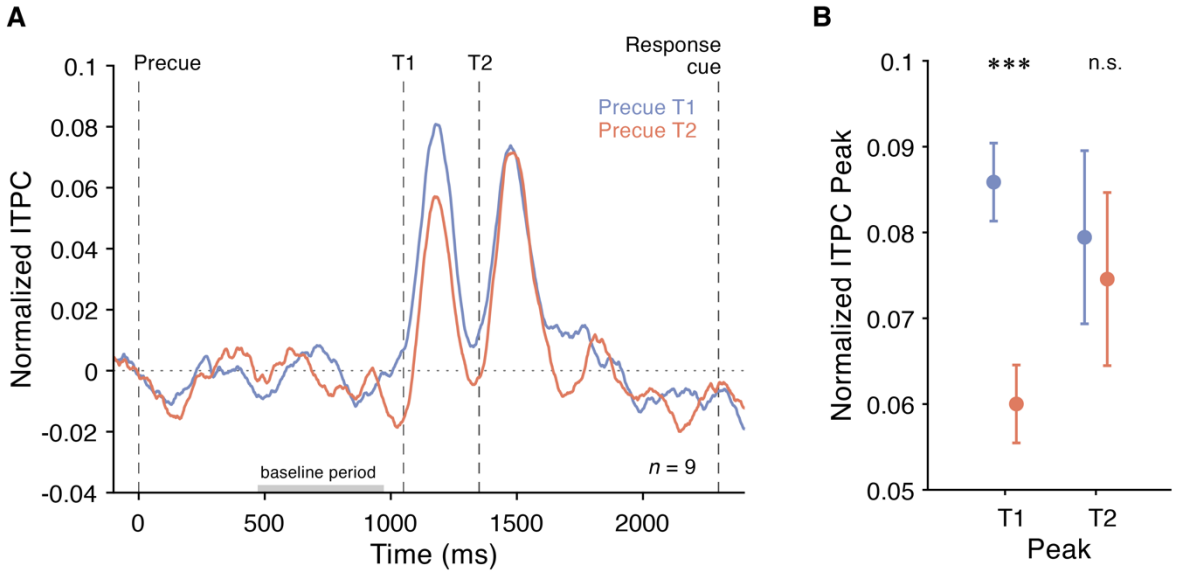


**Figure 6.** Group normalized ITPC. (**A**) Group normalized 20 Hz ITPC time series for each precue condition. Gray bar indicates the 500 ms baseline period used for normalization. (**B**) Effect of temporal attention on normalized target-evoked ITPC responses measured at individual observer peak times. Temporal attention increased the target-evoked ITPC response for T1. Error bars indicate ±1 SED. *** $p < 0.001$.

The magnitude of the target-evoked ITPC response to T1 was larger when T1 was precued than when T2 was precued. To quantify the magnitude of this difference, we measured the peak of the normalized target-evoked ITPC response for each individual observer for the two precue types (see Methods). We found that temporal attention increased the target-evoked ITPC response to T1 ($F(1,8) = 32.34$, $p = 0.0004$, $= 0.23$; precue T1: mean = 0.086, SD = 0.088; precue T2: mean = 0.060, SD = 0.083 (**Figure 6B**). We found no significant effect of the precue on the response to T2 ($F(1,8) = 0.23$, $p = 0.64$, $= 0.005$; precue T1: mean = 0.079, SD = 0.086; precue T2: mean = 0.075, SD = 0.088). The presence of an effect of the precue for T1 and absence for T2 was reflected in a significant interaction of target and validity ($F(1,8) = 7.17$, $p = 0.028$, $= 0.055$). See **Supplementary Table 1** for all ANOVA results for the target-evoked response analyses.

We further investigated the effect of the precue on other measures of the evoked response to the targets. At the same peak times, trial-average normalized SSVER power behaved similarly to ITPC, whereas single-trial normalized 20 Hz power was unrelated to precue validity (**Supplementary Table 1**). Specifically, temporal attention increased the trial-average normalized SSVER power in response to T1 ($F(1,8) = 5.80$, $p = 0.043$, $= 0.11$; precue T1: mean = 560 $fT^2$, SD = 560 $fT^2$; precue T2 mean = 407 $fT^2$, SD = 454 $fT^2$) but not T2 ($F(1,8) = 0.22$, $p = 0.65$, $= 0.0026$; precue T1: mean = 406 $fT^2$, SD = 487 $fT^2$; precue T2 mean = 377 $fT^2$, SD = 497 $fT^2$, **Supplementary Figure 1H**). Single-trial normalized 20 Hz power, in contrast, showed no effect of precue for either target ($F(1,8) < 2.05$, $p > 0.19$, **Supplementary Figure 1I**), demonstrating that the change in ITPC was not driven by a change in 20 Hz power regardless of phase. Finally, we confirmed that the ITPC effect for T1 was specific to 20 Hz (**Supplementary Figure 2**). Therefore, directing temporal attention to the first target changed the steady-state response to that target in a transient fashion.

## Discussion

Temporal attention affected cortical response reliability both in anticipation of and in response to target stimuli. Visual response reliability slowly ramped up as target onset approached, an overall effect of temporal expectation linked to the predictable timing of the target stimuli. Over and above this effect of temporal expectation, temporal attention, reflecting the task relevance of targets at specific times, changed the rate of pre-target ramping and led to transient changes in target-evoked responses.

### Effects of temporal expectation

Previous studies of temporal expectation have found anticipatory ramps in EEG voltage known as the contingent negative variation (CNV), often when a speeded response to a target was required (*1*, *2*, *32*–*35*). The CNV is usually associated with response preparation or interval timing (*36*) and has been localized to frontal and parietal areas (*37*). Ramping activity in motor and parietal areas has also been observed leading up to timed movements (*24*, *38*). Here, instead we found expectation-related ramping in the reliability of stimulus-specific sensory responses, measured by ITPC.

A few studies have found expectation-related modulations of visual areas. In two studies, temporal expectations interacted with spatial (*10*) or feature-based (*39*) attention, such that attentional modulation of visual responses in V4 or V1, respectively, was larger at times when targets were expected. Another study found that temporal expectations led to alpha reductions and gamma increases in macaque V1 in response to irrelevant gratings (*27*). Gamma ramped up over the course of ~1 s before the expected target time. All of these previous studies employed speeded change detection tasks, leaving open the possibility that the cortical modulations were associated with response preparation (*2*). In our task, responses were not made until after the response cue, ruling out this possibility.

One previous study has investigated temporal expectation using SSVER, with mixed results (*40*). This study found post-target increases in SSVER amplitude for predictable vs. unpredictable stimuli for some flicker frequencies, but reversed effects at other flicker frequencies and in the harmonics, with variable dynamics. No increase in SSVER amplitude in advance of a predictable target time emerged. However, the SSVER stimulus had no spatial overlap with the target location, so any expectation-related modulation specific to the target location would not have been visible in the SSVER signal.

SSVER studies of spatial attention sustained across seconds have reported SSVER amplitudes that are relatively constant across a trial (*28*, *29*). This finding suggests that the ramping pattern we observed is specific to situations when the observer has a temporal expectation of a predictable target onset. Future studies using time-resolved SSVER should further investigate what kinds of anticipatory and preparatory processes drive ramping increases in cortical response reliability.

### Effects of temporal attention

Critically, as in our previous studies (*6*–*8*, *22*), our task allowed us to measure specific effects of temporal attention to task-relevant time points, over and above the effects of temporal expectation due to predictable stimulus timing. Our normalization model of dynamic attention predicts that temporal attention will modulate sensory responses (*6*). Based on fits to psychophysical data, the model also predicts that the effects of temporal attention on neural gain will be transient and roughly coincident with the sensory responses.

The current data are consistent with both model predictions: sensory modulation by temporal attention and modulation at a transient timescale. Specifically, the model predicts a change in gain at the neuronal level, which requires a linking hypothesis to make predictions for MEG measures. Gain increases would increase the probability or rate of neuronal spiking in response to each stimulus flicker, which in turn would be expected to lead to more reliable population responses to the SSVER stimulus across trials and thus higher ITPC. However, such a mechanism also might be expected to increase single-trial power, which we did not observe. One possible resolution is that gain increases did occur, but stimulus-driven 20 Hz activity entrained or otherwise interacted with ongoing endogenous (non-phase locked) 20 Hz power, which would be consistent with the low SNR we observed for single-trial power at 20 Hz. Alternatively, it could be the case that changes in ITPC arose from a mechanism other than gain changes, such as more consistent timing of stimulus-driven responses without changes in neuronal response amplitude. Invasive recordings and perhaps modeling efforts could distinguish between these possibilities.

This linking hypothesis between gain increases at the neuronal level and ITPC increases in the SSVER can account for the pre-target effects of attention and expectation we observed, as well as post-target effects for those observers showing a transient increase of the ITPC following each target. However, transient reductions of the ITPC in response to target stimuli, regardless of attention (**Supplementary Text**), appear to arise from observer-specific interactions between the ongoing SSVER and target-evoked responses and are thus not predictable from the normalization model of dynamic attention, which does not include specific biophysical structure.

The current results also reveal an effect of temporal attention not predicted by the model: a modulation of the rate of anticipatory ramping in sensory reliability over the 1 s leading up to stimulus onset. It is not surprising that the model did not predict anticipatory ramping, because the behavioral data alone could not distinguish anticipatory from stimulus and post-stimulus processing; future versions of the model should incorporate these new experimental findings. Interestingly, an overall effect of temporal expectation that is modulated by temporal attention is similar to the pattern we have observed for microsaccades, which also provide continuous measures of anticipatory processes (*22*).

Effects of temporal cueing on early evoked visual responses have also been observed in previous studies, which measured changes in EEG amplitude (*41*) or multi-unit activity in IT (*42*) within 100 ms post-stimulus. However, these studies could not assess whether this sensory modulation was truly transient, as there was no visual stimulation (and thus no stimulus-driven activity) before or after the targets. Moreover, in these studies only a single target was presented on each trial, so temporal attention and expectation could not be disentangled.

Our two-target design allowed us to measure how temporal attention affected evoked responses to both T1 and T2 and to distinguish those effects from temporal expectation. In experimental designs with one target occurring at an expected or unexpected time, observers can reorient to a later time if a target does not appear at an earlier time (*9*, *43*). This reorienting strategy is not possible with two targets and a response cue, because observers must wait for the response cue to find out which target to report. Here we found that temporal attention affected the evoked ITPC response only to T1 and not to T2. We also found only a marginal effect (statistical trend) of temporal attention on T2 *d'*, so it may be that the effect of temporal attention on target processing was generally weaker for T2 than T1. Another possibility, albeit speculative, is that because of the directionality of time, the neural mechanisms of temporal attention differ for T1 and T2. For example, if the pre-target ramping we observed before T1 is causally related to the neural response to the target, this mechanism would be able to impact T1 but not T2. It may be that at early sensory stages, changing the relative responses to the two targets by modulating T1 alone

is sufficient to bias downstream competition between the two target representations and produce attentional tradeoffs in behavior. In our data, the ITPC response to T2 is lower than the T1 response on precue T1 trials but higher on precue T2 trials, consistent with a relative modulation of target responses by attention.

**ITPC as a measure of cortical response reliability**

We quantified cortical response reliability to periodic visual stimulation using ITPC, a measure of phase consistency across trials. Many previous studies using steady state methods have measured the strength of sensory responses using the power of the SSVER signal (at the stimulus frequency) computed from the average time series across trials, i.e., the trial-average SSVER power (*44–46*). Here we focused on ITPC because it is more specific than the trial-average power, which depends on both phase consistency across trials (ITPC) and power at the stimulus frequency on single trials. Studies that have pulled apart ITPC and single-trial power found that trial-average SSVER power is mainly driven by ITPC (*28*, *29*, *31*), with ~70% of the signal variance explained by ITPC and only ~10% explained by single-trial power (*30*). Consistent with these observations, we found that trial-average power was similar to ITPC and that temporal attention and expectation affected ITPC but not single-trial power at the SSVER frequency.

Spatial attention increases ITPC, which has been interpreted as arising from an increase in the synchronization of neurons (*28*, *29*). It is important to distinguish synchronization of a neural population within a trial, which would be expected to increase single-trial SSVER power, from neural synchronization across trials, which would be expected to increase ITPC. Here we adopt a descriptive approach, interpreting ITPC as a measure of response reliability to the visual flicker: a stimulus that more reliably drives the neural response will yield a higher phase coherence across trials (*29*, *31*, *47*). Further, given that the ITPC signal and attention-related modulations were narrow-band at the stimulus frequency of 20 Hz and phase-locked to the stimulus, it is likely that these measurements reflect neural responses driven by the stimulus flicker rather than endogenously generated activity in the beta band.

**Limitations of the study**

A limitation of our approach of characterizing the ramping activity with linear fits is that the ITPC ramps may not be strictly linear. This possibility was hinted at by the group ITPC time series for each precue condition, which looked like they could have periodic modulations. Alternatively, apparent deviations from linearity could be due to noise. In an exploratory analysis, we investigated possible periodicities in the precue-to-T1 interval but failed to find reliable evidence for periodic modulations across observers, leading us to use a simple linear fit. The present results, then, indicate that there is a difference between temporal attention conditions in the linear component of the SSVER signal as the presentation of the first target approaches.

Finally, the interpretation of the attentional modulation of the transient, target-evoked SSVER response is somewhat limited. Although temporal attention increased the impact of the targets on the SSVER for all observers, the targets themselves enhanced the SSVER for some observers and disrupted it for others. This directionality was stable across sessions for each observer. To our knowledge this individual variation is an unexplained observation in the field that deserves further study (**Supplementary Text**). Nevertheless, the current findings show that SSVER can be used to study time-varying cognitive processes locked to brief stimuli, and not only stable “steady state” signals, if the responses are characterized for each observer.

## Conclusions

Using time-resolved SSVER, we studied how voluntary attention to points in time continuously impacts the reliability of cortical responses to visual stimulation. Our measurements revealed two complementary neural mechanisms of temporal attention: (1) a slow, pre-target ramping of visual cortical ITPC that anticipated predictable target times and was modulated by which time point was to be attended, and (2) a transient, post-target increase of the evoked ITPC response to targets at attended time points, which was specific to the first target. This transient modulation changed the relative strengths of the two target responses as a function of attention. These findings help reconcile previous neural findings showing expectation-related ramps in fronto-parietal areas and theoretical work predicting transient post-target changes in visual responses. By revealing the full timecourse of temporal attentional modulations of sensory activity, the results show how attention dynamically alters visual signals to select and prioritize visual information at precise moments in time.

## Methods

### Observers

Ten observers (5 females), ages 24-35 years (M = 28.5 years, SD = 4.2 years) participated, including authors RND and KT. Each observer completed two MEG sessions, which allowed us to check for consistency across sessions for each observer while collecting 20 sessions of MEG data in total, comparable to previous MEG studies of vision (*48*, *49*). The sample size was also similar to previous temporal attention studies that measured accuracy (*3*, *7*, *8*) and to several studies on spatial attention (*50–52*). All observers provided informed consent, and the University Committee on Activities involving Human Subjects at New York University approved the experimental protocols. All observers had normal or corrected-to-normal vision.

### Stimuli

Stimuli were generated on an Apple iMac using MATLAB and Psychophysics Toolbox (*53*, *54*) and were displayed using a gamma-corrected InFocus LP850 projector (Texas Instruments, Warren, NJ) with a resolution of 1024 x 768 pixels and a refresh rate of 60 Hz. Stimuli were projected via a mirror onto a translucent screen at a viewing distance of 42 cm. Stimulus timing accuracy was confirmed with photodiode measurements. Stimuli were presented on a medium gray background (206 cd/m$^2$). A central fixation circle subtended 0.15° visual angle.

**SSVER stimulus.** Throughout the trial, a 20 Hz contrast-reversing flickering noise patch was presented foveally, with the fixation circle overlaid. The noise patch was 4° in diameter with a blurred outer edge subtending 0.4°, fading to the background gray. To create the noise patch, pixel noise was generated from a normal distribution then bandpass filtered in both orientation and spatial frequency around target values: in orientation 0° ± 5° and 90° ± 5° forming a vertical and horizontal crosshatch pattern, and in spatial frequency 1.5 cpd ± 1 octave. A new noise patch was randomly generated on each trial and then flickered throughout the trial with a duty cycle of 33% (1 frame of the original noise image in alternation with 2 frames of the contrast-reversed image). The contrast of the SSVER stimulus was adjusted to ensure high visibility of the target stimuli while still producing a clear SSVER signal (40-55% noise patch contrast across observers).

**Targets.** Visual targets were 1.5 cpd sinusoidal gratings of 4° in diameter with a blurred outer edge subtending 0.4°. Targets were also presented foveally and were added pixelwise to the noise patch stimulus. To match the temporal frequency of the targets to the SSVER stimulus, the targets were also contrast-reversed for 2 cycles at 20 Hz, in phase with the noise patch flicker,

for a total target duration of 100 ms. Target grating contrast was adjusted so that, when added to the noise patch, the total contrast was 100% (grating contrast 45-60% across observers).

**Cues.** Auditory cues were pure sine wave tones 100 ms in duration (with 10 ms cosine amplitude modulation ramps at onset and offset) presented through earbuds at a comfortable volume. There were two possible auditory cue tones, one high-pitched (1046.5 Hz, C6) and one low-pitched (440 Hz, A4).

**Experimental procedure**

All observers participated in two 2-hour MEG sessions on separate days, on average 3.6 days apart. Each session included 12 experimental blocks approximately 6 minutes each in duration. Observers took breaks between blocks and pressed a button to indicate their readiness for the next block.

**Task.** On each trial, observers were asked to discriminate the orientation of one of two grating targets (**Figure 1**). The two targets (T1 and T2) were each presented for 100 ms, separated by a stimulus onset asynchrony (SOA) of 300 ms, based on previous psychophysical studies (*6–8*). Each target was tilted slightly clockwise (CW) or counterclockwise (CCW) from either the vertical or horizontal axis, with independent tilts and axes for T1 and T2. Both vertical and horizontal axes were used to reduce the number of trials on which the two stimuli were identical and discourage observers from adopting a strategy of judging whether the stimuli were the same or different to aid in discrimination. An auditory precue 1,050 ms before the first target instructed observers to attend to the first or the second target (high tone: attend T1; low tone: attend T2). An auditory response cue 950 ms after T2 indicated which of the two targets' tilt to report (high tone: report T1; low tone: report T2). Observers pressed one of two buttons to indicate whether the tilt was CW or CCW relative to the main axis within a 1600 ms response window. The response cue matched the precue on 75% of the trials (valid trials) and mismatched the precue on the remaining 25% (invalid trials). At the end of each trial, feedback was provided by a change in color of the fixation circle (green: correct; red: incorrect; blue: response timeout). At the end of each block, performance accuracy (percent correct) was displayed. The timing of auditory and visual events was the same on every trial. From trial to trial, the allocation of temporal attention varied (depending on the precue), and the response selection varied (depending on the response cue).

So that only the precue would provide predictive timing information about the target onsets, and to allow time for the SSVER signal to stabilize before any trial events occurred, the interval between the SSVER onset and the precue was jittered from 500 to 1500 ms in steps of 200 ms. Between each trial, an inter-trial interval of 1500 ms was presented, during which only the fixation circle appeared on a gray background. Observers were encouraged to blink during this period. The fixation circle turned black at the start of the ITI, turned white 500 ms before the SSVER onset to indicate that the trial was about to begin, and remained white throughout the trial until the response feedback was provided.

Each session consisted of 12 blocks of 41 trials each with all combinations of cue type (valid: 75%, invalid: 25%), probed target (T1, T2), target tilt (CW, CCW; independent for T1 and T2), and target axis (horizontal, vertical; independent for T1 and T2) in a randomly shuffled order. To reduce adaptation to the SSVER stimulus, every fifth trial was a blank trial, with an additional blank trial at the beginning of each block. This procedure yielded a total of 768 temporal attention trials per observer across the two sessions.

**Training and thresholding.** Prior to MEG, observers completed at least one session of training to familiarize them with the task and to determine their orientation tilt thresholds. During the training session, a chin-and-head rest was used to hold head position and viewing distance

constant. Stimuli were displayed on a gamma-corrected Sony Trinitron G520 CRT monitor with a refresh rate of 60 Hz at a viewing distance of 57 cm. A 3-up-1-down staircase procedure was used to estimate each observer's tilt threshold to achieve ~79% accuracy across all trials. Threshold tilts ranged from 1.5-5°.

**Eyetracking.** Eye position was recorded using an EyeLink 1000 eye tracker (SR Research) with a sampling rate of 1000 Hz. Raw gaze positions were converted into degrees of visual angle using the five-point-grid calibration, which was performed at the start of each MEG session.

**MEG recording.** Data were recorded continuously in each block with a 157-channel axial gradiometer system (Kanazawa Institute of Technology, Kanazawa, Japan) in the KIT/NYU facility at New York University. The magnetic fields were sampled at 1000 Hz with online DC filtering and a 200 Hz low-pass filter. Three orthogonally-oriented reference magnetometers placed approximately 20 cm away from the recording array recorded environmental noise.

Before recording, each observer's head shape was digitized with a handheld FastSCAN laser scanner (Polhemus, VT, USA). Digital markers were placed on the forehead, nasion, and left and right tragus and peri-auricular points. To record marker locations with respect to the MEG channels, electrodes were placed on five of the locations identified by the digital markers (three points on the forehead and left and right peri-auricular points), and marker locations were measured at the beginning and end of the MEG recording session.

**Data analysis**

**Preprocessing.** Data was preprocessed in MATLAB using the FieldTrip toolbox for EEG/MEG-analysis (*55*). Environmental noise was removed from the data by regressing signals recorded from three orthogonally oriented magnetometers against the recorded data.

MEG channels in which there was no signal or excessive noise were interpolated from neighboring channels (the number of interpolated channels per recorded session ranged from 2 to 16 (1.3-10.2%), mean = 3.9 (2.5%), SD = 3.0. Trials were manually inspected and rejected for blinks and other artifacts. The number of rejected trials per session ranged from 26 to 73 (5.3-14.8%), mean = 45.4 (9.2%), SD = 14.3.

**Channel selection.** We selected visually responsive channels as the five channels per session with the strongest 20 Hz trial-average SSVER power. Topographies confirmed selected channels were in the posterior part of the head.

**SSVER analysis.** For the SSVER analyses, trials were epoched from 1500 ms before to 5200 ms after the precue. Time-frequency representations of the data were computed using wavelet convolution with the FieldTrip toolbox. For the 20 Hz SSVER frequency, Morlet wavelets had 8 cycles (127 ms temporal resolution, 5 Hz spectral resolution). For full time-frequency spectra, frequency was sampled every 1 Hz from 1-50 Hz, time was sampled every 10 ms, wavelets were tapered with Hanning windows, and the time windows scaled with frequency according to 10 s divided by the frequency.

**Trial-average power.** Trial-average power quantifies the power of a periodic signal that is phase-locked across trials and so survives averaging across trials. This measure has been commonly used in the SSVER literature (*44*, *56*–*58*). To calculate the trial-average power, the time series of all trials (or all trials in a given experimental condition) were first averaged together, giving the mean time series across trials. Time-frequency analysis was then performed on this single time series to calculate the power across time at a frequency of interest. Trial-average power depends on two factors: single-trial power and ITPC.

**Single-trial power.** Single-trial power quantifies the power of a periodic signal present on individual trials. To calculate the single-trial power, time-frequency analysis was performed on each individual trial, and these time-frequency representations were then averaged together across trials. This procedure preserves oscillatory activity that is not phase-locked across trials but relies on having sufficient signal-to-noise at the single trial level to measure the periodic signal.

**ITPC.** Inter-trial phase coherence (ITPC) quantifies the phase alignment of a periodic signal across trials. The measure ranges from 0 (no phase alignment) to 1 (perfect phase alignment) (*59*). To calculate ITPC, time-frequency analysis was performed on each individual trial, returning estimates of the instantaneous phase angle at each point in time for a frequency of interest. The following standard formula was then used to calculate the alignment of these phase angles across trials, providing an estimate of ITPC:

$$ITPC_{tf} = \frac{1}{N}\left|\sum_{n=1}^{N} e^{i\phi_{tf}}\right|$$

Where $\phi_{tf}$ is the instantaneous phase angle in radians at a time point $t$ and frequency $f$ for each trial $n \in [1,\ldots,N]$.

**Slope analysis.** To quantify the pre-target ITPC ramping rate for individual observers, we fit lines to the ITPC time series in the time window between the precue and first target. In all trials, a predictable interval of 1.05 s elapsed between the onset of the precue and the onset of T1, so observers could form an expectation about the timing of T1 onset. To prevent T1 from influencing ITPC measurements of pre-target activity due to the temporal bandwidth of the wavelet, we set a cushion before T1 based on the group average ITPC time series across all trials. The start of the cushion was the inflection point 80 ms before T1 when ITPC began to sharply decrease due to the T1 response. Thus the precue-to-T1 window was defined as the onset of the precue to 80 ms before T1.

To assess the overall effect of expectation on ITPC in this precue-to-T1 period, we fit lines to the ITPC time series calculated from all trials. To assess the effect of temporal attention, we fit lines to ITPC time series calculated from trials for each precue condition separately. In all cases, we fit lines for each observer and session and then statistically assessed the slope parameters from these fits.

We also investigated whether there was any basis in the data for assessing periodic activity in the precue-to-T1 period, in addition to a linear ramp. To do so, we performed FFTs of the ITPC time series in this period, both across all trials and split up by precue condition, and assessed the resulting frequency distributions across observers using non-parametric tests. However, we did not find the power in any specific frequency bin (1-20 Hz, 1 Hz resolution) to differ from the null distribution after correcting for multiple comparisons.

**Peak analysis.** To quantify the evoked ITPC response for individual observers, we estimated the latency, direction, and amplitude of the most prominent deflection in the 20 Hz ITPC following each target, which we refer to as a “peak”. As ITPC data in the selected visual channels was highly consistent across sessions for a given observer, we identified peak times for each observer using the ITPC time series averaged across the two sessions. To find the peaks, we applied the MATLAB algorithm *findpeaks.m* to the time window 0 ms to 600 ms after T1 onset, which captured the evoked ITPC responses to both T1 and T2.

All observers but one had two peaks that were either upward or downward during this window. The observer without an identifiable pair of peaks was not considered further in the peak analysis. Two observers had both upward peaks and downward peaks during the window, so for these

observers we selected the pair of peaks whose timing was best aligned with the peaks of the other observers. The direction of the pair of peaks identified by this algorithm determined the classification of an observer as having either upward or downward peaks.

We next assessed the effect of attention on the magnitude of the ITPC peaks, regardless of their direction. To combine evoked ITPC data across observers for this analysis, we first normalized the data so that peaks for all observers pointed upward. To do so, we measured a baseline ITPC value for each observer and session in the window 470-970 ms after the precue (a 500 ms window before target onset, excluding the 80 ms cushion before T1, see "Slope analysis"). We then subtracted that baseline value from the time series, and for observers with downward peaks, reversed the sign:

$$ITPC_{\text{normalized}} = (ITPC - baseline) * s$$

where $s$ = 1 for observers with upward peaks and -1 for observers with downward peaks. This procedure allowed all evoked ITPC peaks to point upward while preserving all other features of the time series.

Finally, to quantify the ITPC magnitude at the peak times, for each observer, session, and precue condition, we took the mean normalized ITPC value in a 100 ms window centered on each peak time (i.e., following each target). Equivalent peak analyses were performed for trial-average 20 Hz power and single-trial 20 Hz power using the same peak times and normalization procedure.

**Statistical analysis.** The effects of temporal attention on behavior (*d'* and RT and MEG time series (slopes and peak values) were assessed using repeated measures ANOVAs via the *ezANOVA* package in R. For behavioral data, the within-subject factors were session, target, and validity (valid or invalid, with respect to the match between the precue and response cue), with session as an observed factor. For MEG slope analyses, within-subject factors were session and precue (precue T1 or precue T2), with session as an observed factor. For MEG peak analyses, within-subject factors were session, target, and attention (attended or unattended, with respect to the precue type, referenced to each target), with session as an observed factor. Planned ANOVAs were also conducted for each target separately.

To assess the effect of the precue on the full time series or time-frequency spectrum, we used a non-parametric test with cluster correction (*60*). This involved a two-step procedure using data averaged across sessions for each observer. In the first step, paired t-tests were performed at each time point or time-frequency bin (henceforth, "bin" for both) comparing precue T1 to precue T2 condition values. This operation yielded t-statistics for each bin for the empirical data. Contiguous bins passing the $p < 0.05$ threshold were considered to form a cluster, and a statistic was generated for each cluster by taking the sum of the t-values for bins within the cluster. The largest statistic out of all clusters was considered to be the maximum cluster statistic for the empirical data. Next, null distributions of the maximum cluster statistic were constructed by shuffling the labels for the precue conditions, computing the maximum cluster statistic for the shuffled data, and repeating this process 1000 times. Significance levels for the empirical data were determined by comparing the value of the maximum cluster statistic to the null distribution.

## Acknowledgements

We thank Sirui Liu and Luis Ramirez for assistance with early versions of the experiment. We thank Hsin-Hung Li, Amit Yashar, and members of the Carrasco and Denison Labs for helpful comments. We thank Jeffrey Walker at the NYU MEG lab for technical assistance.

**Funding:**
National Institutes of Health National Eye Institute R01 EY019691 (MC)
National Institutes of Health National Eye Institute F32 EY025533 (RND)
National Institutes of Health National Eye Institute T32 EY007136 (NYU)
National Defense Science and Engineering Graduate Fellowship (KT)
Boston University (RND)

**Author contributions:**
Conceptualization: RND, DJH, MC
Methodology: RND, KT, DJH, MC
Investigation: RND, KT
Visualization: RND, KT
Supervision: RND, DJH, MC
Writing—original draft: RND, KT
Writing—review & editing: RND, KT, DJH, MC

**Competing interests.** Authors declare they have no competing interests.

**Data and materials availability:** All data are available in the main text or the supplementary materials.

**Supplementary materials:**
Supplementary Text
Tables S1 and S2
Figures S1 to S5

## References


1. C. Miniussi, E. L. Wilding, J. T. Coull, A. C. Nobre, Orienting attention in time: Modulation of brain potentials. *Brain*. 122, 1507–1518 (1999).

2. Á. Correa, J. Lupiáñez, P. Tudela, Attentional preparation based on temporal expectancy modulates processing at the perceptual level. *Psychon B Rev*. 12, 328–334 (2005).

3. K. Davranche, B. Nazarian, F. Vidal, J. Coull, Orienting attention in time activates left intraparietal sulcus for both perceptual and motor task goals. *J Cognitive Neurosci*. 23, 3318–3330 (2011).

4. G. Rohenkohl, I. C. Gould, J. Pessoa, A. C. Nobre, Combining spatial and temporal expectations to improve visual perception. *J Vision*. 14, 8–8 (2014).

5. J. Samaha, P. Bauer, S. Cimaroli, B. R. Postle, Top-down control of the phase of alpha-band oscillations as a mechanism for temporal prediction. *Proc National Acad Sci*. 112, 8439–8444 (2015).

6. R. N. Denison, M. Carrasco, D. J. Heeger, A dynamic normalization model of temporal attention. *Nat Hum Behav*, 1–12 (2021).

7. A. Fernández, R. N. Denison, M. Carrasco, Temporal attention improves perception similarly at foveal and parafoveal locations. *J Vision*. 19, 12–12 (2019).

8. R. N. Denison, D. J. Heeger, M. Carrasco, Attention flexibly trades off across points in time. *Psychon B Rev*. 24, 1142–1151 (2017).

9. A. C. Nobre, F. van Ede, Anticipated moments: Temporal structure in attention. *Nat Rev Neurosci*. 19, 34–48 (2018).

10. G. M. Ghose, J. H. R. Maunsell, Attentional modulation in visual cortex depends on task timing. *Nature*. 419, 616–620 (2002).

11. S. A. Hillyard, E. K. Vogel, S. J. Luck, Sensory gain control (amplification) as a mechanism of selective attention: electrophysiological and neuroimaging evidence. *Philosophical Transactions Royal Soc Lond Ser B Biological Sci*. 353, 1257–1270 (1998).

12. D. Richter, M. Ekman, F. P. de Lange, Suppressed sensory response to predictable object stimuli throughout the ventral visual stream. *J Neurosci*. 38, 7452–7461 (2018).

13. V. Wyart, A. C. Nobre, C. Summerfield, Dissociable prior influences of signal probability and relevance on visual contrast sensitivity. *Proc National Acad Sci*. 109, 3593–3598 (2012).

14. S. Cheadle, T. Egner, V. Wyart, C. Wu, C. Summerfield, Feature expectation heightens visual sensitivity during fine orientation discrimination. *J Vision*. 15, 14 (2015).

15. P. Kok, D. Rahnev, J. F. M. Jehee, H. C. Lau, F. P. de Lange, Attention reverses the effect of prediction in silencing sensory signals. *Cereb Cortex*. 22, 2197–2206 (2012).

16. C. Summerfield, T. Egner, Expectation (and attention) in visual cognition. *Trends Cogn Sci*. 13, 403–409 (2009).

17. C. Summerfield, T. Egner, Feature-based attention and feature-based expectation. *Trends Cogn Sci*. 20, 401–404 (2016).

18. J. W. Bang, D. Rahnev, Stimulus expectation alters decision criterion but not sensory signal in perceptual decision making. *Sci Rep-uk*. 7, 17072 (2017).

19. N. Rungratsameetaweemana, J. T. Serences, Dissociating the impact of attention and expectation on early sensory processing. *Curr Opin Psychology*. 29, 181–186 (2019).

20. A. Todorovic, J.-M. Schoffelen, F. van Ede, E. Maris, F. P. de Lange, Temporal expectation and attention jointly modulate auditory oscillatory activity in the beta band. *Plos One*. 10, e0120288 (2015).

21. K. Lange, B. Röder, Orienting attention to points in time improves stimulus processing both within and across modalities. *J Cognitive Neurosci*. 18, 715–729 (2006).

22. R. N. Denison, S. Yuval-Greenberg, M. Carrasco, Directing voluntary temporal attention increases fixational stability. *J Neurosci*. 39, 353–363 (2019).

23. M. I. Leon, M. N. Shadlen, Representation of time by neurons in the posterior parietal cortex of the macaque. *Neuron*. 38, 317–327 (2003).

24. G. Maimon, J. A. Assad, A cognitive signal for the proactive timing of action in macaque LIP. *Nat Neurosci*. 9, 948–955 (2006).

25. H. Merchant, D. L. Harrington, W. H. Meck, Neural basis of the perception and estimation of time. *Annu Rev Neurosci*. 36, 313–336 (2013).

26. G. T. Finnerty, M. N. Shadlen, M. Jazayeri, A. C. Nobre, D. V. Buonomano, Time in cortical circuits. *J Neurosci*. 35, 13912–13916 (2015).

27. B. Lima, W. Singer, S. Neuenschwander, Gamma responses correlate with temporal expectation in monkey primary visual cortex. *J Neurosci*. 31, 15919–15931 (2011).

28. Y. J. Kim, M. Grabowecky, K. A. Paller, K. Muthu, S. Suzuki, Attention induces synchronization-based response gain in steady-state visual evoked potentials. *Nat Neurosci*. 10, 117–125 (2007).

29. Y. Kashiwase, K. Matsumiya, I. Kuriki, S. Shioiri, Time courses of attentional modulation in neural amplification and synchronization measured with steady-state visual-evoked potentials. *J Cognitive Neurosci*. 24, 1779–1793 (2012).

30. S. Moratti, B. A. Clementz, Y. Gao, T. Ortiz, A. Keil, Neural mechanisms of evoked oscillations: Stability and interaction with transient events. *Hum Brain Mapp*. 28, 1318–1333 (2007).

31. J. Ding, G. Sperling, R. Srinivasan, Attentional modulation of SSVEP power depends on the network tagged by the flicker frequency. *Cereb Cortex*. 16, 1016–1029 (2006).

32. G. Mento, V. Tarantino, A. Vallesi, P. S. Bisiacchi, Spatiotemporal neurodynamics underlying internally and externally driven temporal prediction: A high spatial resolution ERP study. *J Cognitive Neurosci*. 27, 425–439 (2015).

33. A. Breska, R. B. Ivry, Context-specific control over the neural dynamics of temporal attention by the human cerebellum. *Sci Adv*. 6, eabb1141 (2020).

34. G. Walter, R. Cooper, V. J. Aldrige, W. C. McCallum, A. L. Winter, Contingent negative variation: An electric sign of sensorimotor association and expectancy in the human brain. *Nature* (1964) (available at http://kutaslab.ucsd.edu/people/kutas/279/pdfs/1964.N.380.pdf).

35. R. Amit, D. Abeles, M. Carrasco, S. Yuval-Greenberg, Oculomotor inhibition reflects temporal expectations. *Neuroimage*. 184, 279–292 (2019).

36. K. K. Ng, S. Tobin, T. B. Penney, Temporal accumulation and decision processes in the duration bisection task revealed by contingent negative variation. *Frontiers Integr Neurosci*. 5, 77 (2011).

37. G. Mento, The role of the P3 and CNV components in voluntary and automatic temporal orienting: A high spatial-resolution ERP study. *Neuropsychologia*. 107, 31–40 (2017).

38. A. Mita, H. Mushiake, K. Shima, Y. Matsuzaka, J. Tanji, Interval time coding by neurons in the presupplementary and supplementary motor areas. *Nat Neurosci*. 12, 502–507 (2009).

39. S. Warren, E. Yacoub, G. Ghose, Featural and temporal attention selectively enhance task-appropriate representations in human V1. *Nat Commun*. 5, 5643–5643 (2014).

40. A. Mora-Cortes, K. R. Ridderinkhof, M. X. Cohen, Evaluating the feasibility of the steady-state visual evoked potential (SSVEP) to study temporal attention. *Psychophysiology*. 55, e13029 (2017).

41. Á. Correa, J. Lupiáñez, E. Madrid, P. Tudela, Temporal attention enhances early visual processing: A review and new evidence from event-related potentials. *Brain Res*. 1076, 116–128 (2006).

42. B. Anderson, D. L. Sheinberg, Effects of temporal context and temporal expectancy on neural activity in inferior temporal cortex. *Neuropsychologia*. 46, 947–957 (2008).

43. J. T. Coull, A. C. Nobre, Where and when to pay attention: The neural systems for directing attention to spatial locations and to time intervals as revealed by both PET and fMRI. *J Neurosci*. 18, 7426–7435 (1998).

44. S. T. Morgan, J. C. Hansen, S. A. Hillyard, Selective attention to stimulus location modulates the steady-state visual evoked potential. *Proc National Acad Sci*. 93, 4770–4774 (1996).

45. M. M. Müller, W. Teder, S. A. Hillyard, Magnetoencephalographic recording of steadystate visual evoked cortical activity. *Brain Topogr*. 9, 163–168 (1997).

46. S. K. Andersen, M. M. Müller, Behavioral performance follows the time course of neural facilitation and suppression during cued shifts of feature-selective attention. *Proc National Acad Sci*. 107, 13878–13882 (2010).

47. M. Eidelman-Rothman, E. Ben-Simon, D. Freche, A. Keil, T. Hendler, N. Levit-Binnun, Sleepless and desynchronized: Impaired inter trial phase coherence of steady-state potentials following sleep deprivation. *Neuroimage*. 202, 116055 (2019).

48. P. Kok, P. Mostert, F. P. de Lange, Prior expectations induce prestimulus sensory templates. *Proc National Acad Sci*. 114, 10473–10478 (2017).

49. M. W. Flounders, C. González-García, R. Hardstone, B. J. He, Neural dynamics of visual ambiguity resolution by perceptual prior. *Elife*. 8, e41861 (2019).

50. A. Fernández, M. Carrasco, Extinguishing exogenous attention via transcranial magnetic stimulation. *Curr Biol*. 30, 4078-4084.e3 (2020).

51. M. Jigo, M. Carrasco, Differential impact of exogenous and endogenous attention on the contrast sensitivity function across eccentricity. *J Vision*. 20, 11 (2020).

52. K. Anton-Erxleben, K. Herrmann, M. Carrasco, Independent effects of adaptation and attention on perceived speed. *Psychol Sci*. 24, 150–159 (2012).

53. D. H. Brainard, The psychophysics toolbox. *Spatial Vision*. 10, 433–436 (1997).

54. D. G. Pelli, The VideoToolbox software for visual psychophysics: transforming numbers into movies. *Spatial Vision*. 10, 437–442 (1997).

55. R. Oostenveld, P. Fries, E. Maris, J.-M. Schoffelen, FieldTrip: Open source software for advanced analysis of MEG, EEG, and invasive electrophysiological data. *Comput Intel Neurosc*. 2011, 156869 (2011).

56. M. M. Müller, W. Teder-Sälejärvi, S. A. Hillyard, The time course of cortical facilitation during cued shifts of spatial attention. *Nat Neurosci*. 1, 631–634 (1998).

57. M. M. Müller, T. W. Picton, P. Valdes-Sosa, J. Riera, W. A. Teder-Sälejärvi, S. A. Hillyard, Effects of spatial selective attention on the steady-state visual evoked potential in the 20–28 Hz range. *Cognitive Brain Res*. 6, 249–261 (1998).

58. A. M. Norcia, L. G. Appelbaum, J. M. Ales, B. R. Cottereau, B. Rossion, The steady-state visual evoked potential in vision research: A review. *J Vision*. 15, 4 (2015).

59. J. Lachaux, E. Rodriguez, J. Martinerie, F. J. Varela, Measuring phase synchrony in brain signals. *Hum Brain Mapp*. 8, 194–208 (1999).

60. E. Maris, R. Oostenveld, Nonparametric statistical testing of EEG- and MEG-data. *J Neurosci Meth*. 164, 177–190 (2007).

61. M. M. Müller, S. K. Andersen, A. Keil, Time course of competition for visual processing resources between emotional pictures and foreground task. *Cereb Cortex*. 18, 1892–1899 (2008).

62. R. R. Campagnoli, M. J. Wieser, L. F. Gruss, M. R. Boylan, L. M. McTeague, A. Keil, How the visual brain detects emotional changes in facial expressions: Evidence from driven and intrinsic brain oscillations. *Cortex*. 111, 35–50 (2019).

63. R. M. van Diepen, A. Mazaheri, The caveats of observing inter-trial phase-coherence in cognitive neuroscience. *Sci Rep-uk*. 8, 2990 (2018).